Research Article

Asmawi Nazrin, Salit Mohd Sapuan*, Mohamed Yusoff Mohd Zuhri, Intan Syafinaz Mohamed Amin Tawakkal, and Rushdan Ahmad Ilyas

Flammability and physical stability of sugar palm crystalline nanocellulose reinforced thermoplastic sugar palm starch/poly(lactic acid) blend bionanocomposites

https://doi.org/10.1515/ntrev-2022-0007
received September 11, 2021; accepted September 30, 2021

Abstract: In this study, sugar palm crystalline nanocellulose (SPCNC)-reinforced thermoplastic sugar palm starch (TPS) was blended with poly(lactic acid) (PLA) in order to prioritize the biodegradation feature while offsetting individual polymer limitation. Prior to melt blending process, SPCNC was dispersed through sonication in advance of starch gelatinization which was later casted into petri dishes. PLA and TPS were melt blended into five different ratios using Brabender mixer followed by compression molding. Soil degradation (4 months) and water uptake (4 weeks) tests were conducted to evaluate the physical stability of PLA/TPS blend bionanocomposites. Based on Fickian law, the diffusion curve and coefficient of diffusion for seawater, river water, and sewer water were calculated. The flammability and limiting oxygen index (LOI) tests were conducted in accordance with ASTM D635 and ASTM D2863, respectively. For PLA60TPS40 (40% TPS), significant reduction (46–69%) was recorded in maximum water uptake in all mediums, while soil degradation rate experienced insignificant increment (7.92%) for PLA70TPS30 (30% TPS) owing to the reinforcement of SPCNC through the well-dispersed TPS within PLA. Meanwhile, the flammability rates and LOI values for PLA40TPS60 and PLA60TPS40 indicated flammable material properties.

Keywords: bionanocomposites, poly(lactic acid), seawater uptake, soil degradation, thermoplastic starch

* **Corresponding author: Salit Mohd Sapuan,** Laboratory of Biocomposite Technology, Institute of Tropical Forestry and Forest Products (INTROP), Universiti Putra Malaysia, 43400 UPM Serdang, Selangor, Malaysia; Advanced Engineering Materials and Composites Research Centre (AEMC), Department of Mechanical and Manufacturing Engineering, Universiti Putra Malaysia, 43400 UPM Serdang, Selangor, Malaysia, e-mail: sapuan@upm.edu.my
Asmawi Nazrin: Laboratory of Biocomposite Technology, Institute of Tropical Forestry and Forest Products (INTROP), Universiti Putra Malaysia, 43400 UPM Serdang, Selangor, Malaysia
Mohamed Yusoff Mohd Zuhri: Laboratory of Biocomposite Technology, Institute of Tropical Forestry and Forest Products (INTROP), Universiti Putra Malaysia, 43400 UPM Serdang, Selangor, Malaysia; Advanced Engineering Materials and Composites Research Centre (AEMC), Department of Mechanical and Manufacturing Engineering, Universiti Putra Malaysia, 43400 UPM Serdang, Selangor, Malaysia
Intan Syafinaz Mohamed Amin Tawakkal: Department of Process and Food Engineering, Universiti Putra Malaysia, 43400 UPM Serdang, Selangor, Malaysia
Rushdan Ahmad Ilyas: School of Chemical and Energy Engineering, Faculty of Engineering, Universiti Teknologi Malaysia, 81310 Johor Bahru, Johor, Malaysia; Centre for Advanced Composite Materials (CACM), Universiti Teknologi Malaysia (UTM), Johor Bahru, 81310 Johor, Malaysia

1 Introduction

Non-biodegradable petrochemical-based plastics are polluting the environment at a concerning rate instigating long term environmental, economic, and waste management problems [1]. The effort to dispose and recycle plastic wastes are inefficient due to poor management, high recycling cost, and difficulties in polymer separation, which end up either in landfills or the ocean [2]. Finite petroleum resources coupled with the rising environmental issues had prompted scientists and material engineers to shift toward biodegradable food packaging materials derived from bioresources as an alternative replacement for current conventional plastics [3]. PLA is a promising biodegradable polymer synthesized from bioresources with unique features such as glossy appearance, decent transparency, good processability, and high rigidity [4]. However, PLA exhibits slow degradation rate in soil and little to no degradation in seawater [5]. In soil,

PLA films with thickness of 0.2 mm exhibited no mass loss at 25 and 37°C after 1 year, but 40% mass loss was detected at 45°C after 8 weeks [2]. PLA showed no mass loss in seawater and fresh water under simulated conditions over 1 year. In sewage sludge, the biological degradation (CO_2 release) of PLA was 43% at 37°C after 277 days [6] and 75% at 55°C after 75 days [7].

In an effort to solve the marine plastic waste pollution, starch is incorporated to induce biodegradation, while reducing the raw material cost of PLA. Starch had piqued the interest of fellow researchers in manufacturing of food packaging plastics due to their promising features such as colorless, odorless, tasteless, non-toxic, and biodegradable properties [8]. Several modifications have been carried out in order to improve their mechanical strength, water barrier, and thermal properties such as plasticizers addition, fiber reinforcement, and polymer blending. Sugar palm starch (SPS) like most starches has received considerable research attention in developing biodegradable food packaging materials. Its high amylose content (37%) was reported as a good film-forming material in producing starch biopolymer films comparable to other commercial starches [9]. Sanyang *et al.* [10] reported that SPS films plasticized by sorbitol achieved 28.35 MPa in tensile strength, while the one plasticized by glycerol reached 61.63% in elongation at break. Prominently, nanosized fibers have gained tremendous attraction due to their outstanding features, such as excellent mechanical properties, light weight, low density, high surface area (100 m^2/g), and high aspect ratio of 100 compared to other commercial fibers [11]. Ilyas *et al.* [12] reported SPS biocomposite film reinforced with 0.5% sugar palm crystalline nanocellulose (SPCNC) which demonstrated an improvement in both tensile strength (140%) and water vapor permeability (19.94%). However, starch-based biocomposite deteriorates its mechanical strength easily upon prolonged exposure to moisture. Hence, blending with hydrophobic polymer such as poly(lactic acid) (PLA) helps to offset the low water barrier properties of starch-based biocomposite. The incorporation of low-cost starch filler will inevitably deteriorate mechanical strength, but at the same time induce water absorption for microorganism inhabitation to enhance degradability in aqueous environments [13].

In this context, PLA is blended with SPCNC-reinforced thermoplastic sugar palm starch (TPS) in an effort to overcome individual polymer limitations and achieve desirable material properties for intended application. To date, only limited research has been conducted on the water uptake within seawater, river water, and sewer water. To the best of authors' knowledge, there have been no study performed on water uptake of seawater, river water, and sewer water for polymer blend composites of PLA with SPCNC-reinforced TPS. TPS and SPCNC have similar botanical origin with similar chemical composition forming good compatibility between fibers and matrixes. In the present study, PLA/TPS blend bionanocomposites were fabricated into five different ratios and the capabilities of each composition was evaluated based on their flammability behavior, soil degradation behavior as well as water uptake of seawater, river water, and sewer water.

2 Materials and methods

2.1 Materials

SPS in the form of mixture of starch and woody fibers extracted from the trunk of sugar palm tree was purchased from Hafiz Adha Enterprise at Kampung Kuala Jempol, Negeri Sembilan, Malaysia. PLA (NatureWork 2003D), glycerol, and sorbitol were bought from Mecha Solve Engineering, Petaling Jaya, Malaysia. SPCNC derived from sugar palm fibers which are naturally entwined at the outer part of sugar palm tree was provided by Laboratory of Biocomposite Technology, Institute of Tropical Forestry and Forest Products, Universiti Putra Malaysia, Selangor, Malaysia. Table 1 shows the physical properties of SPCNC and their values.

2.2 Extraction and preparation of SPS

SPS was extracted from the trunk of sugar palm trees located at Jempol, Negeri Sembilan, Malaysia. Initially, the mixture of starch and woody fibers were transferred into a bucket and left out for 1 day for the sedimentation of starch while less dense fibers floated to the surface. The floating fibers were removed and a strainer cloth was

Table 1: Physical properties of SPCNC and their values

Properties	Value
Density (g/cm^3)	1.05
Diameter (nm)	9
Surface area (m^2/g)	14.47
Pore volume (cm^3/g)	0.226
Moisture content (wt%)	17.90
Molecular weight (g/mol)	23164.7
Degree of crystallinity (%)	85.9
Degree of polymerization	142.86

Table 2: Various composition of PLA/TPS blend bionanocomposites

Designation	PLA (%)	TPS (%)
PLA20TPS80	20	80
PLA40TPS60	40	60
PLA60TPS40	60	40
PLA70TPS30	70	30
PLA80TPS20	80	20
PLA100	100	0

used to filter finer size woody fiber residue mixed with starch. Next the wet starch was spread evenly onto a plastic film and left in open air for a moment. Then, the starch was transferred into an air circulating oven at 120°C for 24 h to obtain starch powder. The extraction method was adapted from Sahari *et al.* [14].

2.3 Fabrication of SPCNC-reinforced TPS/PLA blend bionanocomposite sheets

Solution casting method was used to fabricate TPS. Initially, 1,000 mL of distilled water was filled in a beaker and 0.5 g SPCNC (0.5%), 15 g of both glycerol (15%) and sorbitol (15%) were added. Sonication method was applied for 15 min to agitate SPCNC to ensure discontinuous particles distribution and uniform dispersion in the liquid. Then, the beaker was transferred into a water bath with a temperature of 80°C. Progressively, 100 g SPS was added into the mixture, while maintaining continuous stirring for 30–45 min until a semi-fluid consistency was attained. The gelatinized starch was transferred into glass petri dishes and placed in an oven for drying at 60°C for 24 h. Later, the dried-up gelatinized starch formed thin TPS films and were crushed into granule-size to ease the melt blending process. PLA granules and crushed TPS films were melt blended using Brabender Plastograph (Model 815651, Brabender GmbH & Co. KG, Duisburg, Germany) at 170°C for 13 min with a rotor speed of 50 rpm. PLA and TPS were blended into five different ratios of 20:80, 40:60, 60:40, 70:30, and 80:20. Once again, the blend bionanocomposites were crushed into granule-size before being hot pressed (Technovation, Selangor, Malaysia) at 170°C for 17 min into 150 mm × 150 mm × 3 mm sheet. Table 2 shows the composition of PLA/TPS blend bionanocomposites. Figure 1 shows the overall preparation of PLA/TPS blend bionanocomposites.

2.4 Flammability test

Flammability test was conducted in accordance with ASTM D635 in a horizontal position. Prior to the test, samples (125 mm × 13 mm × 3 mm) were placed in an oven for 24 h at 100°C to remove remaining moisture. Two reference lines were drawn at distances of 25 mm and 100 mm as starting and finishing marks. Then, the sample was clamped horizontally at the end side leaving both reference lines visible using retort stand. The sample was lit at the other end side and as soon as the flame reached a distance of 25 mm, the timer was started. The test was carried out in triplicate and time taken for the flame to reach 100 mm was recorded. The burning rate of the sample can be calculated using equation (1):

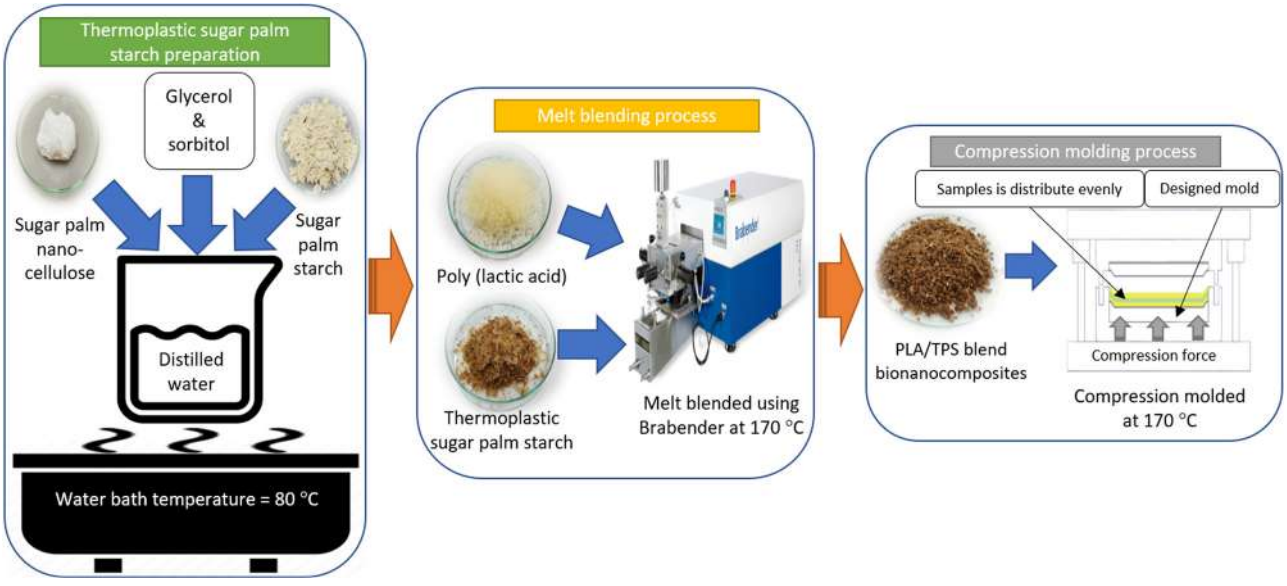

Figure 1: Schematic diagram of the preparation of PLA/TPS blend bionanocomposites.

$$V = \frac{L}{t}, \tag{1}$$

where V is the linear burning rate (mm/min), L is the burnt length (mm), and t is the time (min)

2.5 Limiting oxygen index (LOI)

The LOI test was conducted in accordance with ASTM D2863 to measure the lowest oxygen concentration for combustion of a sample. Prior to the test, samples (100 mm × 6.5 mm × 3 mm) were placed in an oven for 24 h at 100°C to remove remaining moisture. The sample was clamped vertically in the glass chamber and lit up for 10 s until ignition. Figure 2 shows the experimental setup of LOI test. The test was carried out with ten replicate samples. The LOI value can be calculated using equation (2):

$$\text{LOI (vol\%)} = \text{Cf} + kd, \tag{2}$$

where Cf is the final value of oxygen concentration in vol% for the previous five measurements, d is the interval difference in vol% between oxygen concentration levels (0.2 vol%), and k is the factor derived from the experimental value.

2.6 Biodegradation in compost soil

Six samples (15 mm × 15 mm × 3 mm) were buried in polybags containing characterized soil at 10 cm depth, which was moistened daily with water. Plastic mesh was used to wrap the samples before burying into the soil to facilitate removal of the degraded samples while maintaining the access of moisture and microorganism. The physiochemical properties of the soil were pH: 6; organic carbon: 35%; total nitrogen: 1.3%; phosphorus: 1,750 ppm; potassium: 1,750 ppm; magnesium: 2,500 ppm; and calcium: 4,500 ppm. Prior to testing, samples were dried at 100°C for 24 h and weighed to obtain the initial weight, W_i. Four sets of experiments were made for predetermined 1 month interval for 4 months. Samples were taken from the soil at specified intervals and gently cleaned with distilled water to remove impurities. Finally, samples were left to dry at 100°C for 24 h and weighed to obtain the final weight, W_f. The test was done in triplicate and the average values were taken. The weight loss, W_l can be calculated using equation (3):

$$W_l = \frac{W_i - W_f}{W_i} \times 100\%. \tag{3}$$

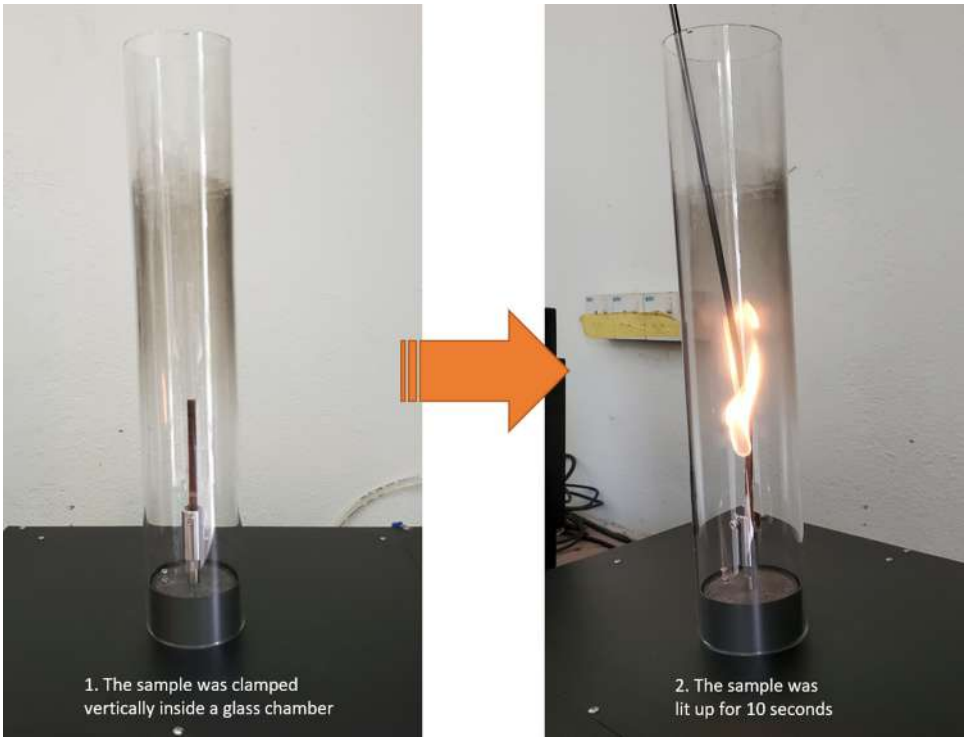

Figure 2: The experimental setup of LOI test.

Table 3: Origin sources of seawater, river water, and sewer water

Medium	Source (coordinate)
Seawater	Shoreline of Malacca Strait (2°54′54.2″N 101°19′15.9″E)
River water	Kuyoh river of pale brown water (3°00′51.6″N 101°43′07.7″E)
Sewer water	Seri Serdang town with less than 10 building blocks (3°00′35.2″N 101°42′49.2″E)

2.7 Water uptake

Total of six samples (20 mm × 15 mm × 3 mm) were immersed in three different conditions which were seawater, river water, and sewer water. Table 3 shows the origin sources of the three different mediums used in this study. Prior to testing, samples were dried at 100°C for 24 h and weighed to obtain the initial weight, W_0. After selected immersion periods, the samples were removed, washed, wiped, and weighed (W_t) using OHAUS balance with a precision of 1 mg at room temperature (25°C and RH 25%). The test was done in triplicate and the average values were taken. The percentage of weight gain at given time M_t can be calculated using equation (4):

$$M_t = \frac{W_t - W_0}{W_t} \times 100\%. \tag{4}$$

The test was done in triplicate and the maximum moisture absorption, M_{max}, was calculated as an average value with very little variation in water uptake. The weight gained from moisture absorption can be modeled in terms of two parameters, the diffusion coefficient D and M_{max}, and are given by Fick's first law in equation (5):

$$\frac{M_t}{M_{max}} = 1 - \frac{8}{\pi^2} \sum \frac{1}{(2n+1)^2} \exp\left(-\frac{D(2n+1)^2\pi^2 t}{h^2}\right), \tag{5}$$

where h is the thickness of the sample and D can be calculated using the initial linear portion of the absorption curve. For $M_t/M_{max} \leq 0.5$, the function $M_t = f(\sqrt{t})$ is linear and the Fickian diffusion coefficient D is determined by equation (6):

$$D = \frac{\pi}{16}\frac{h^2}{t}\left(\frac{M_t}{M_{max}}\right)^2. \tag{6}$$

As this equation is commonly used in square specimen dimension, a correction factor is required to interpret for the finite length l and width w of the sample compared to its thickness h using equation (7):

$$\mathrm{Dc} = D\left(1 + \frac{d}{l} + \frac{d}{w}\right)^{-2}. \tag{7}$$

3 Results and discussion

3.1 Flammability test

The flammability behavior of a material are attributed to its chemical composition and interfacial bonding formed within the material itself [15]. The chemical composition of the plastic cause ease in ignition when exposed to sufficient heat in the presence of oxygen. In an effort to minimize the flammability of plastic, implementation of additional flame retardant materials or substances had been utilized. Table 4 shows the effect of blending TPS with PLA at various ratios toward their burning rate and behavior. As observed, the introduction of TPS into PLA induced flammability in the blend bionanocomposite samples but only for PLA60TPS40 and PLA40TPS60, while the flame for PLA80TPS20, PLA70TPS30, and PLA20TPS80 quickly extinguished before reaching the first 25 mm reference line. PLA60TPS40 and PLA40TPS60 continuously burned till 100 mm reference line indicating highly flammable properties. This is mainly caused by the incorporated plasticizers in fabricating TPS which are glycerol and sorbitol. Glycerol and sorbitol are known to be flammable substances with the flash point of 176 and above 300°C,

Table 4: Burning rate, UL94 rating, and burning behavior of pristine PLA and PLA/TPS blend bionanocomposites

Sample	Burning rate	Burning behavior	LOI (vol%)
PLA20TPS80	Inflammable	Partially burned, slow dripping, moderate smoke, and low flame	—
PLA40TPS60	16.39 mm/min (HB)	Fully burned, fast dripping, less smoke, and low flame	19.2%
PLA60TPS40	15.29 mm/min (HB)	Fully burned, fast dripping, less smoke, and low flame	18.8%
PLA70TPS30	Inflammable	Partially burned, moderate dripping, moderate smoke, and moderate flame	—
PLA80TPS20	Inflammable	Partially burned, moderate dripping, moderate smoke, and moderate flame	—
PLA100	Inflammable	Partially burned, moderate dripping, moderate smoke, and moderate flame	—

respectively [16]. The higher concentration of plasticizers in TPS seemed to greatly affect the burning rate as can be seen for PLA40TPS60 (16.39 mm/min) which exhibited faster burning rate compared to PLA60TPS40 (15.29 mm/min). This occurrence can be associated with the migration of glycerol from TPS into PLA due to its lower molecular weight which activated the flammability in the PLA phase. Various authors [17–19] reported that during the melt mixing process, lower molecular weight of glycerol (92 g/mol) tends to migrate from TPS to PLA matrix, while higher molecular weight sorbitol (182 g/mol) stayed within TPS. Sorbitol is responsible for decreasing the particle size and promoted a fine dispersion of TPS within PLA phase resulting in homogeneous composition. The uniform distribution of TPS within PLA triggered a continuous combustion of the samples. Even so, the burning rate of PLA40TPS60 and PLA60TPS40 were less than 40 mm/min which classified as HB in UL94 rating. In other words, they are considered to be the least flame retardant material that required improvement in flammability features. Due to this fact, some researchers [20,21] substituted glycerol with glycerol phosphate with the intention of increasing the flame retardant properties of starch-based polymer blend.

According to our previous paper [22], the scanning electron microscope (SEM) image of PLA60TPS40 displayed smooth surface morphology indicating good interfacial bonding, while some visible agglomeration spots of TPS were detected for PLA40TPS60 and PLA20TPS80. All these samples showed a constant dripping of the melted material. Meanwhile, PLA80TPS20 and PLA70TPS30 displayed some microcracks and voids indicating poor interfacial bonding between PLA and TPS. It was observed that when these two samples lit up, fragment of material was detached rather than a consistent dripping. The minor proportion of TPS within the samples melted quickly as compared to less flammable PLA phase which led to the detachment of PLA fragment with the assistance of spread microcracks. Based on those behaviors, it was verified that PLA60TPS40 and PLA40TPS60 have the optimal plasticizers concentration to promote the flammability of PLA and improve the dispersion of TPS into PLA. Nazrin *et al.* [19] conducted Dynamic Mechanical Analysis and reported a significant increment in storage modulus for PLA60TPS40 (53.5%), while trivial changes were recorded for PLA70TPS30 (10%) and PLA80TPS20 (0.6%) due to the insufficient glycerol migration to promote the chain mobility responsible in improving the storage modulus.

Based on Table 4, PLA40TPS60 (19.2%) had a slightly higher LOI value compared to PLA60TPS40 (18.8%). Bocz *et al.* [20] recorded the LOI value of 22% for TPS plasticized with 25% glycerol and 21% for PLA/TPS plasticized with 5% glycerol. This verified that the higher content of TPS required higher oxygen concentration for combustion although higher concentration of glycerol was incorporated. This might be the reason as why PLA20TPS80 was not flammable as PLA40TPS60 and PLA60TPS40 even though it undoubtedly consisted the highest glycerol concentration among all the blend bionanocomposite samples. Relatively higher TPS content indicated higher concentration of SPCNC within the samples. Supposedly, lignin content within cellulose generated char formulation which helps to hinder flame propagation [21]. However, the removal of lignin in order to produce low water retention of SPCNC might have induced the flammability rate for sample with higher TPS content [23]. However, the effect of glycerol migration overwhelms the SPCNC reinforcement.

3.2 Soil burial: weight loss

The calculation of weight loss during soil burial test was done by observing the biodegradation behaviors of a material. The weight loss of the blend bionanocomposites is due to consumption of starch by microorganisms. Figure 3 shows an increasing trend of the percentage of weight loss as the addition of TPS was increased within the blend. In the first 30 days, all blend bionanocomposites went through active degradation process and for the next 90 days, lower degradation rates were recorded. Amylopectin residing within the blend consists of branched hydroxylated chains, which promote hydration and water diffusion resulting in microorganisms growth [24]. The reduction in degradation rate can be associated with the adaptation of microorganisms to the materials after colonization. Ohkita and Lee [25] fabricated PLA/TPS (70:30 and 50:50) blend composites with and without the incorporation of lysine diisocyanate (LDI) as a coupling agent and recorded that the samples with LDI had a steady weight loss for 1 month, while those without LDI had a significant degradation rate for 1 week. LDI acts as a coupling agent by removing the hydroxyl groups of PLA and TPS, thus lowering the accessibility for microorganisms' invasion.

In similar case, Ayana *et al.* [26] found that priorly dispersed montmorillonite clays (1 PHR) during starch gelatinization and later melt mixed with PLA (PLA/TPS, 40:60) promoted the compatibility between immiscible polymer blends by reducing the size distribution of the PLA in the starch matrix. The exfoliation of clay nanolayers established a tortuous path preventing further water penetration into the PLA/TPS blend nanocomposites. The

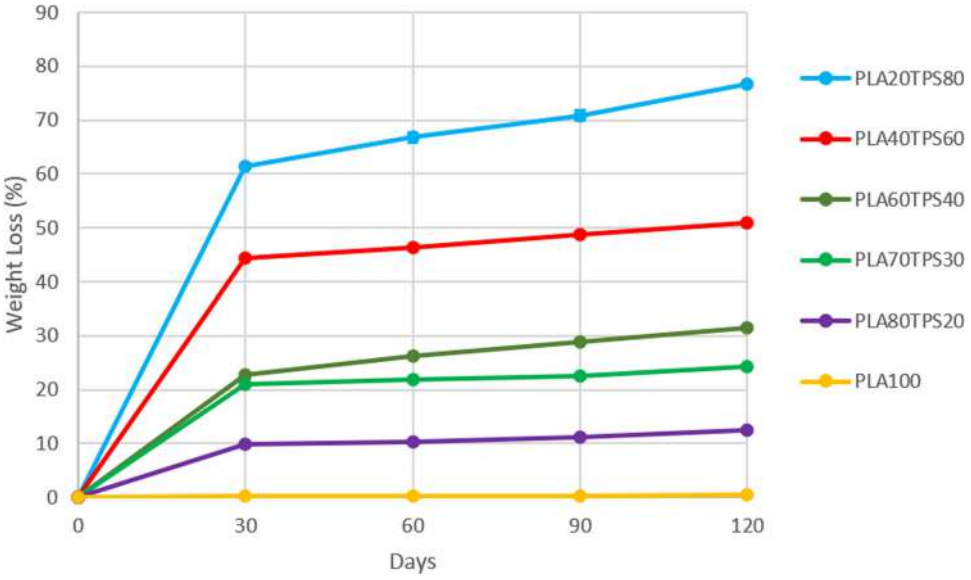

Figure 3: Weight loss against time of PLA100 and PLA/TPS blend bionanocomposites.

dispersion of SPCNC within TPS for all the blend bionanocomposites seemed to play the exact role as nanoclays to establish tortuous path hindering water penetration for microorganisms to inhabit [27]; though, this mechanism can work only if homogenous combination between PLA and TPS was achieved. Within the first 30 days, a minor increase in weight loss was recorded between PLA70TPS30 (20.92%) and PLA60TPS40 (22.72%). In relation to flammability results, the homogenous composition achieved at PLA60TPS40 seemed to prevent rapid degradation of TPS phase. Taking into account the dispersion of SPCNC, the water penetration into the sample was reduced resulting in lower microorganism inhabitation. Other samples experienced significant increase as TPS content was increased. At 60% of TPS content (PLA40TPS60) (44.45%), the weight loss increased significantly as compared to PLA60TPS40 (20.92%). The agglomeration spots presented in PLA40TPS60 and PLA20TPS80 as mentioned in Section 3.1 acted as an active spot for microorganisms' inhabitation which led to rapid degradation. The physical condition of these two samples were observed to be completely shrunk into smaller pieces after 24 h of oven drying process. Meanwhile, PLA60TPS40, PLA70TPS30, and PLA80TPS20 seemed to maintain their physical shape with some visible cavities on the surface due to degradation of the TPS.

PLA100 did not seem to experience degradation process as no weight loss was recorded. Another factor which might be affecting the degradation rate was the plasticizers used. Sanyang *et al.* [10] reported that sorbitol-plasticized TPS had lower water vapor transmission rate compared to glycerol-plasticized TPS. The migration of glycerol from TPS into PLA led to a lower moisture content for all the samples. Lower moisture content caused compact hydrogen bonds interaction between starch and water suggesting that a high number of free hydroxyl groups of the starch are available to interact with the active sites of sorbitol. Hence, the chances of sorbitol interacting with water molecules become lower.

3.3 Water uptake

All bionanocomposite samples including pristine PLA (PLA100) were immersed in three type of liquid medium which are seawater, river water, and sewer waste water. The water uptake of all bionanocomposite samples is solely contributed by TPS content as PLA is well-known for its strong hydrophobic nature. Based on Table 5, the reduction in TPS content decreases the equilibrium water content of the blend bionanocomposites regardless of the medium used. The sample with highest TPS content (PLA20TPS80) had the highest value of equilibrium water content. There are several factors that influenced the water absorption of a polymer composite which are diffusivity, exposed surface area, permeability, temperature, surface protection, fiber content, and orientation [12]. In this study, temperature was kept constant at room temperature (25 ± 1°C) and uniform exposed surface area through fixed sample size with no incorporation of surface protection was considered. As the composition of each sample was different, fiber content and orientation are expected to be different. The differences between the

Table 5: Equilibrium water content (M_{max}), coefficient of diffusion (D), and corrected coefficient of diffusion (Dc) of pristine PLA and PLA/TPS blend bionanocomposites within seawater, river water, and sewer water

Medium	Seawater			River water			Sewer water		
Sample	M_{max} (%)	$D{\cdot}10^{-6}$ (cm^2/s)	$Dc{\cdot}10^{-6}$ (cm^2/s)	M_{max} (%)	$D{\cdot}10^{-6}$ (cm^2/s)	$Dc{\cdot}10^{-6}$ (cm^2/s)	M_{max} (%)	$D{\cdot}10^{-6}$ (cm^2/s)	$Dc{\cdot}10^{-6}$ (cm^2/s)
PLA20TPS80	18.37	2.45	1.35	17.87	2.45	1.35	20.24	4.91	2.69
PLA40TPS60	20.02	0.41	0.22	16.08	0.41	0.22	14.88	0.41	0.22
PLA60TPS40	6.08	1.23	0.67	8.68	1.23	0.67	6.34	1.23	0.67
PLA70TPS30	8.35	0.41	0.22	7.51	0.41	0.22	7.44	1.23	0.67
PLA80TPS20	6.22	0.41	0.22	5.7	0.41	0.22	7.68	0.21	0.11
PLA100	0	0	0	0	0	0	0	0	0

orientation can be observed from the SEM analysis of the previous paper [22], where slight agglomeration spots can be observed within samples that have TPS content more than 40% (PLA20TPS80 and PLA40TPS60), while microcracks and voids are presented within samples that have TPS content lower than 40% (PLA70TPS30 and PLA80TPS20).

Strangely, PLA40TPS60 has a lower coefficient of diffusion value compared to PLA60TPS40 within all mediums. This might be due to the high concentration of SPCNC within the sample which might hinder the diffusivity of the water molecules. Ilyas *et al.* [12] reported that the incorporation of 0.5% SPCNC into sugar palm starch biocomposite films reduced the equilibrium water

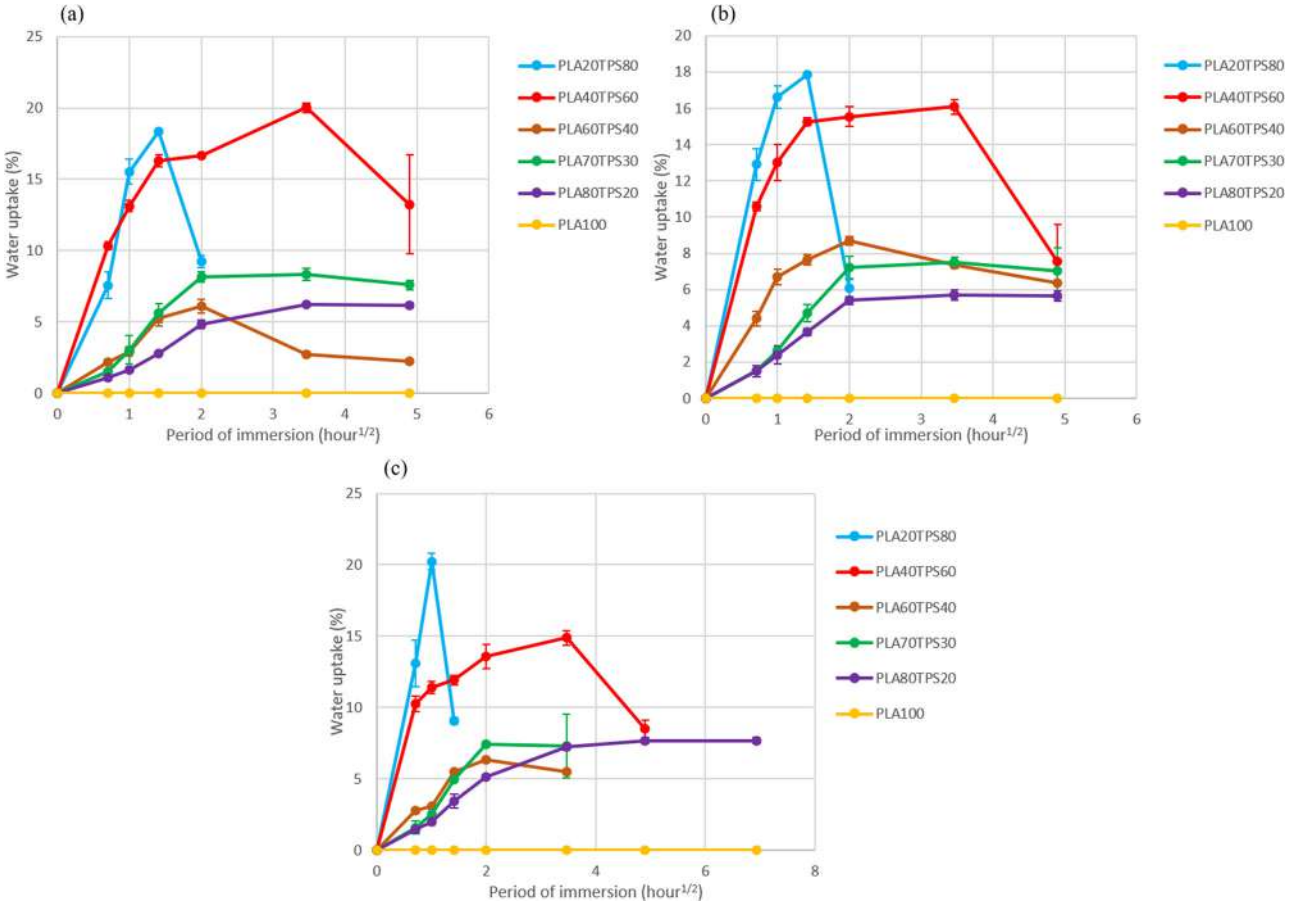

Figure 4: The water uptake (%) against period of immersion (hour$^{1/2}$) of PLA100 and PLA/TPS blend bionanocomposites within: (a) seawater, (b) river water, and (c) sewer water.

sorption by 16%. The decrement in the coefficient of diffusion for PLA40TPS60 can be attributed to the high crystallization of SPCNC [28]. For PLA60TPS40, the sample has a better compatibility between PLA and TPS, thus promoting uniform distribution of water molecules in TPS well-dispersed within PLA. This led to quicker diffusivity of water molecules into the samples but at the same time reducing equilibrium water content [27]. Apart from that, PLA20TPS80 displayed higher coefficient of diffusion in sewer water compared to seawater and river water. It is speculated that the static condition of sewer water might be the cause of the high coefficient of diffusion. Continuous flow of seawater and river water stimulate the circulation of foreign particles while procuring them as compared to sewer water which remained static.

The movement of water molecules into polymer composites are based on three mechanisms [29]: diffusion, capillary movement, and transport of water molecules. Diffusion occurs inside the free volume (micro gaps) between polymer chains. Capillary transport occurs through capillary connection through the gaps and cracks at the interface between fibers and continuous phase. Transport of water molecules occurs due to the swelling of fiber within the matrix. Based on Figure 4, sample with highest TPS content reached equilibrium water uptake quickly compared with lower content of TPS regardless of the medium used. The highest value of equilibrium water uptake did not exceed 20% for all samples, while for PLA60TPS40, a significant drop of equilibrium water content can be observed within all medium of immersion with seawater having the lowest value which is 6.08%. It was reported [30] that the seawater contained various minerals (up to 3.5%) which limited the diffusion of water molecules into the polymer composite materials. Based on the previous paper [22], water uptake of the PLA60TPS40 within distilled water reached up to 25% for only 2 h of immersion period. The absence of components such as minerals facilitate the diffusivity of water molecules. In the seawater medium, it is observed that PLA40TPS60 (20.02%) had a slightly higher equilibrium water content value compared to PLA20TPS80 (18.37%). Since the coefficient of diffusion for PLA40TPS60 within all mediums were the same, the difference was insignificant considering the large standard deviation displayed in Figure 4. It was suspected that some replicates might have higher TPS content due to the poor compatibility resulting in extra agglomeration spots. As soon as PLA20TPS80 and PLA40TPS60 reached equilibrium water content, the water uptake dropped rapidly. It was observed that these two samples experienced defragmentation due to the higher TPS content validating the poor physical stability correlated with the results from soil degradation.

4 Conclusion

In a nutshell, the reinforcement of SPCNC within the blend bionanocomposites could only be optimized if TPS is well-dispersed within PLA phase. In order to achieve such condition, a harmonize ratio between PLA and TPS must be identified. The maximum water uptake within seawater, river water, and sewer water decreased as TPS content decreased, but only PLA60TPS40 displayed a significant reduction compared to other samples. However, the coefficient of diffusion recorded a higher value for PLA60TPS40 compared to PLA40TPS60 and PLA70TPS30 owing to uniform distribution of water molecules within the well dispersed TPS within PLA leading to a quicker diffusivity but reducing maximum water uptake. The soil degradation rate also showed minor change between PLA70TPS30 and PLA60TPS40 compared to PLA60TPS40 and PLA40TPS60 due to the tortuous path of SPCNC hindering water penetration for microorganisms to inhabit. PLA60TPS40 and PLA40TPS60 demonstrated burning rate lower than 40 mm/min which were classified as HB in UL94 rating and considered as least flame retardant material. Meanwhile, the low LOI values of PLA40TPS60 (19.2%) and PLA60TPS40 (18.8%) indicated that they were highly flammable materials within atmospheric air. In food packaging application that prioritize biodegradability and cheap material, PLA60TPS40 demonstrated tolerable physical stability but required improvement in flame retardant features.

Funding information: The authors wish to thank Universiti Putra Malaysia for the financial support through Inisiatif Pemerkasaan Penerbitan Jurnal Tahun 2020 (Vot number: 9044033) and Geran Putra Berimpak (GPB), UPM/800-3/3/1/GPB/2019/9679800.

Author contributions: All authors have accepted responsibility for the entire content of this manuscript and approved its submission.

Conflict of interest: The authors state no conflict of interest.

References

[1] Castro-Aguirre E, Iñiguez-Franco F, Samsudin H, Fang X, Auras R. Poly(lactic acid) – mass production, processing, industrial applications, and end of life. Adv Drug Deliv Rev. Dec. 2016;107:333–66. doi: 10.1016/j.addr.2016.03.010.

[2] Kliem S, Kreutzbruck M, Bonten C. Review on the biological degradation of polymers in various environments. Materials (Basel). 2020;13(20):1–18. doi: 10.3390/ma13204586.

[3] Nurazzi NM, Asyraf MRM, Khalina A, Abdullah N, Aisyah HA, Ayu Rafiqah S, et al. A review on natural fiber reinforced polymer composite for bullet proof and ballistic applications. Polymers (Basel). Feb. 2021;13(4):646. doi: 10.3390/polym13040646.
[4] Siakeng R, Jawaid M, Asim M, Siengchin S. Accelerated weathering and soil burial effect on biodegradability, colour and textureof coir/pineapple leaf fibres/PLA biocomposites. Polymers (Basel). Feb. 2020;12(2):458. doi: 10.3390/polym12020458.
[5] Wang GX, Huang D, Ji JH, Völker C, Wurm FR. Seawater-degradable polymers – fighting the marine plastic pollution. Adv Sci. 2021;8(1):1–26. doi: 10.1002/advs.202001121.
[6] Yagi H, Ninomiya F, Funabashi M, Kunioka M. Mesophilic anaerobic biodegradation test and analysis of eubacteria and archaea involved in anaerobic biodegradation of four specified biodegradable polyesters. Polym Degrad Stab. 2014;110:278–83. doi: 10.1016/j.polymdegradstab.2014.08.031.
[7] Yagi H, Ninomiya F, Funabashi M, Kunioka M. Thermophilic anaerobic biodegradation test and analysis of eubacteria involved in anaerobic biodegradation of four specified biodegradable polyesters. Polym Degrad Stab. 2013;98(6):1182–7. doi: 10.1016/j.polymdegradstab.2013.03.010.
[8] Hazrati KZ, Sapuan SM, Zuhri MYM, Jumaidin R. Effect of plasticizers on physical, thermal, and tensile properties of thermoplastic films based on Dioscorea hispida starch. Int J Biol Macromol. Jun. 2021;185:1–33. doi: 10.1016/j.ijbiomac.2021.06.099.
[9] Ilyas RA, Sapuan SM, Atiqah A, Ibrahim R, Abral H, Ishak MR, et al. Sugar palm (Arenga pinnata [Wurmb.] Merr) starch films containing sugar palm nanofibrillated cellulose as reinforcement: water barrier properties. Polym Compos. July 2019;121:1–9. doi: 10.1002/pc.25379.
[10] Sanyang ML, Sapuan SM, Jawaid M, Ishak MR, Sahari J. Effect of plasticizer type and concentration on tensile, thermal and barrier properties of biodegradable films based on sugar palm (Arenga pinnata) starch. Polymers (Basel). 2015;7(6):1106–24. doi: 10.3390/polym7061106.
[11] Norrrahim MNF, Ariffin H, Yasim-Anuar TAT, Hassan MA, Ibrahim NA, Yunus WMZW, et al. Performance evaluation of cellulose nanofiber with residual hemicellulose as a nanofiller in polypropylene-based nanocomposite. Polymers (Basel). Mar. 2021;13(7):1064. doi: 10.3390/polym13071064.
[12] Ilyas RA, Sapuan SM, Ishak MR, Zainudin ES. Development and characterization of sugar palm nanocrystalline cellulose reinforced sugar palm starch bionanocomposites. Carbohydr Polym. Dec. 2018;202:186–202. doi: 10.1016/j.carbpol.2018.09.002.
[13] Huang D, Hu ZD, Liu TY, Lu B, Zhen ZC, Wang GX, et al. Seawater degradation of PLA accelerated by water-soluble PVA. E-Polymers. 2020;20(1):759–72. doi: 10.1515/epoly-2020-0071.
[14] Sahari J, Sapuan SM, Zainudin ES, Maleque MA. Thermo-mechanical behaviors of thermoplastic starch derived from sugar palm tree (Arenga pinnata). Carbohydr Polym. Feb. 2013;92(2):1711–6. doi: 10.1016/j.carbpol.2012.11.031.
[15] Ratnavathi CV, Patil JV, Chavan UD. Sorghum biochemistry: An industrial perspective. Cambridge, MA: Academic Press; 2016.
[16] Sherwani SFK, Zainudin ES, Sapuan SM, Leman Z, Abdan K. Mechanical properties of sugar palm (Arenga pinnata Wurmb. Merr)/glass fiber-reinforced poly(lactic acid) hybrid composites for potential use in motorcycle components. Polymers (Basel); 2021;13(18):3061. doi: 10.3390/polym13183061.
[17] Li H, Huneault MA. Comparison of sorbitol and glycerol as plasticizers for thermoplastic starch in TPS/PLA blends. J Appl Polym Sci. Feb. 2011;119(4):2439–48. doi: 10.1002/app.32956.
[18] Esmaeili M, Pircheraghi G, Bagheri R, Altstädt V. Poly(lactic acid)/coplasticized thermoplastic starch blend: effect of plasticizer migration on rheological and mechanical properties. Polym Adv Technol. 2019;30(4):839–51. doi: 10.1002/pat.4517.
[19] Nazrin A, Sapuan SM, Zuhri MYM, Tawakkal ISMA, Ilyas RA. Water barrier and mechanical properties of sugar palm crystalline nanocellulose reinforced thermoplastic sugar palm starch (TPS)/poly(lactic acid) (PLA) blend bionanocomposites. Nanotechnol Rev. Jun. 2021;10(1):431–42. doi: 10.1515/ntrev-2021-0033.
[20] Bocz K, Szolnoki B, Marosi A, Tábi T, Wladyka-Przybylak M, Marosi G. Flax fibre reinforced PLA/TPS biocomposites flame retarded with multifunctional additive system. Polym Degrad Stab. 2014;106:63–73. doi: 10.1016/j.polymdegradstab.2013.10.025.
[21] Sienkiewicz A, Czub P. Flame retardancy of biobased composites – research development. Materials (Basel). 2020;13(22):1–30. doi: 10.3390/ma13225253.
[22] Nazrin A, Sapuan SM, Zuhri MYM. Mechanical, physical and thermal properties of sugar palm nanocellulose reinforced thermoplastic starch (tps)/poly(lactic acid) (PLA) blend bionanocomposites. Polymers (Basel). Sep. 2020;12(10):2216. doi: 10.3390/polym12102216.
[23] Kim NK, Dutta S, Bhattacharyya D. A review of flammability of natural fibre reinforced polymeric composites. Compos Sci Technol. 2018;162:64–78. doi: 10.1016/j.compscitech.2018.04.016.
[24] Rodrigues CA, Tofanello A, Nantes IL, Rosa DS. Biological oxidative mechanisms for degradation of poly(lactic acid) blended with thermoplastic starch. ACS Sustain Chem Eng. 2015;3(11):2756–66. doi: 10.1021/acssuschemeng.5b00639.
[25] Ohkita T, Lee SH. Thermal degradation and biodegradability of poly(lactic acid)/corn starch biocomposites. J Appl Polym Sci. 2006;100(4):3009–17. doi: 10.1002/app.23425.
[26] Ayana B, Suin S, Khatua BB. Highly exfoliated eco-friendly thermoplastic starch (TPS)/poly(lactic acid)(PLA)/clay nanocomposites using unmodified nanoclay. Carbohydr Polym. Sep. 2014;110:430–9. doi: 10.1016/j.carbpol.2014.04.024.
[27] Nor Arman NS, Chen RS, Ahmad S. Review of state-of-the-art studies on the water absorption capacity of agricultural fiber-reinforced polymer composites for sustainable construction. Constr Build Mater. July 2021;302:124174. doi: 10.1016/j.conbuildmat.2021.124174.
[28] Petchwattana N, Sanetuntikul J, Sriromreun P, Narupai B. Wood plastic composites prepared from biodegradable poly (butylene succinate) and burma padauk sawdust (pterocarpus macrocarpus): water absorption kinetics and sunlight exposure investigations. J Bionic Eng. 2017;14(4):781–90. doi: 10.1016/S1672-6529(16)60443-2.
[29] Muñoz E, García-Manrique JA. Water absorption behaviour and its effect on the mechanical properties of flax fibre reinforced bioepoxy composites. Int J Polym Sci. 2015;2015:1–10. doi: 10.1155/2015/390275.
[30] Deroiné M, Le Duigou A, Corre YM, Le Gac PY, Davies P, César G, et al. Accelerated ageing of polylactide in aqueous environments: comparative study between distilled water and seawater. Polym Degrad Stab. 2014;108:319–29. doi: 10.1016/j.polymdegradstab.2014.01.020.